Engineered nanoparticles interacting with cells: size matters

Li Shang[1], Karin Nienhaus[1] and Gerd Ulrich Nienhaus[1,2,3*]

Abstract

With the rapid advancement of nanoscience and nanotechnology, detailed knowledge of interactions between engineered nanomaterials and cells, tissues and organisms has become increasingly important, especially in regard to possible hazards to human health. This review intends to give an overview of current research on nano-bio interactions, with a focus on the effects of NP size on their interactions with live cells. We summarize common techniques to characterize NP size, highlight recent work on the impact of NP size on active and passive cellular internalization and intracellular localization. Cytotoxic effects are also discussed.

Keywords: Nanoparticle, Cellular uptake, Protein corona, Endocytosis, Red blood cell, Cytotoxicity

Introduction

In recent years, nanoparticles (NPs) and other nanomaterials have entered essentially all areas of our everyday lives. In industrial applications, they have become indispensable components of catalysts [1], sensors [2] or photovoltaic devices [3]. In the biomedical field, they have found wide-spread use as nanovaccines [4], nanodrugs [5] and diagnostic imaging tools [6]. However, our knowledge about biological effects and, importantly, potential risks of the omnipresent (intended and unintended) exposure to nanomaterials has not kept up with the pace of these developments and is still very limited [7,8].

NPs may invade the human body via inhalation, ingestion or through the skin (Figure 1). Once they have entered a biological milieu, NPs will inevitably come into contact with a huge variety of biomolecules including proteins, sugars and lipids that are dissolved in body fluids, such as the interstitial fluid between cells, lymph or blood. These biomolecules immediately coat the NP surfaces and form the so-called 'protein corona' [9-11], which determines the biological identity of the NP [12]. Its composition is dynamic and depends on the relative concentrations of the individual components and on their affinities toward the NP surface. In fact, NPs have to be viewed as evolving systems that adapt to varying concentrations of the biomolecules present in the fluid. It has been suggested that the 'final corona' reflects its own prior history [13].

NPs have to surmount the cell membrane to intrude cells. One of the hallmarks of any cell membrane is its ability to selectively control the flow of ions and molecules into and out of the cell, and to maintain a separation between the cytosol and the extracellular environment. Large macromolecular agglomerates, e.g., protein assemblies, lipoprotein particles, viruses and also NPs are typically encapsulated in vesicles and selectively transported into and out of the cells via endocytosis and exocytosis, respectively (Figure 1). Different types of endocytosis mechanisms are known, varying with the size of the transport vesicle, cargo properties and the internalization machinery involved. In most cells, internalization occurs via pinocytosis. In this process, an invagination forms in the cell membrane that is finally pinched off so as to generate a vesicle in the cytoplasm that contains the internalized materials. Typically, the inward budding vesicles contain receptor proteins that recognize specific chemical groups on the molecules to be internalized. Thus, if proteins adsorbed to an NP trigger cell surface receptors, they will readily activate the cell's uptake machinery, whereas adsorbed proteins that only weakly interact with membrane-associated biomolecules will reduce the uptake of the 'disguised' NPs. Specialized cells, so-

* Correspondence: uli.nienhaus@kit.edu
[1]Institute of Applied Physics and Center for Functional Nanostructures (CFN), Karlsruhe Institute of Technology (KIT), Wolfgang-Gaede-Strasse 1, 76131 Karlsruhe, Germany
[2]Institute of Toxicology and Genetics (ITG), Karlsruhe Institute of Technology (KIT), Hermann-von-Helmholtz-Platz 1, 76344 Eggenstein-Leopoldshafen, Germany
Full list of author information is available at the end of the article
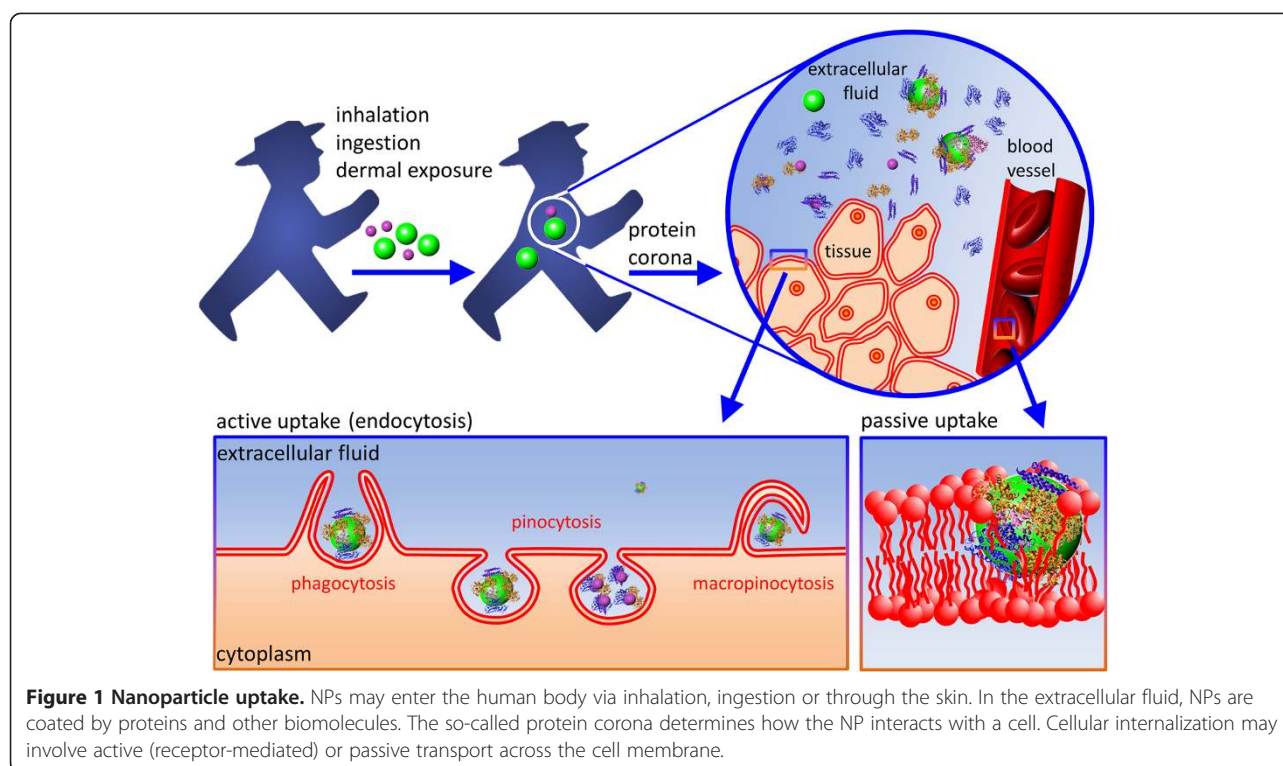
Figure 1 Nanoparticle uptake. NPs may enter the human body via inhalation, ingestion or through the skin. In the extracellular fluid, NPs are coated by proteins and other biomolecules. The so-called protein corona determines how the NP interacts with a cell. Cellular internalization may involve active (receptor-mediated) or passive transport across the cell membrane.

called 'professional phagocytes,' such as macrophages, neutrophils, and monocytes are capable of phagocytosis, a form of endocytosis in which the cell engulfs larger particles. In addition to intruding cells by active transport, NPs may also enter cells by passive penetration of the cell membrane. In fact, for cells lacking the endocytosis machinery such as red blood cells (RBCs), passive transport is the only option.

Regardless of the specific internalization mechanism, the cell-NP interactions are, on the one hand, modulated by physicochemical properties of the NPs including size, shape, surface charge and surface chemistry [14] and, on the other hand, by cell-specific parameters such as cell type or cell cycle phase [15]. The uptake efficiency might even be affected by specific properties of the experimental setup [16]. A quantitative understanding of the NP-biomolecule/membrane interaction is, therefore, an important prerequisite for designing and engineering NPs with intentionally enhanced or suppressed cellular uptake [17,18]. In the present review, we shall focus mainly on the effect of NP size on the interaction with live cells. We present a survey of methods to determine the size of NPs, investigate the impact of the NP size on active and passive uptake and discuss their cytotoxic effects.

Characterization of the NP size in biological media

To correlate a particular physicochemical property of a NP with biological responses and to ensure that these results are reproducible and meaningful, an accurate characterization of the NP is essential. NP size is a key parameter (in the following, particle size always refers to the diameter). Many NPs are composed of a 'heavy' core (*e.g.,* a metal or semiconductor nanocrystal) surrounded by small organic ligands to ensure colloidal stability. Electron microscopy techniques such as transmission electron microscopy (TEM) can easily provide accurate size measurements with sub-nanometer resolution. However, organic surface ligands are difficult to resolve owing to their low electron density, so the TEM-determined size mainly reflects the size of the core. In addition, the requirement of high vacuum for TEM imaging calls for complicated sample preparation procedures that can result in NP aggregation [19]. Dynamic light scattering (DLS) is a widely used technique for NP size determination in suspension. DLS is based on scattering intensity fluctuations due to Brownian motion of NPs in suspension and relates the diffusion coefficient to the size *via* the Stokes–Einstein equation. The measured hydrodynamic diameter reflects the dimension of the NP (core plus shell) together with layer of surface-bound solvent. DLS provides a simple and speedy measurement of NP size in biological media. However, the method suffers from low sensitivity toward small particles and possible interference from light-absorbing species [20]. Fluorescence correlation spectroscopy (FCS) is a sensitive technique capable of measuring the hydrodynamic diameter of freely diffusing NPs, if these are either intrinsically fluorescent or have been labeled with fluorescent dyes [9]. The FCS method is based on the analysis

of the duration of brief bursts of photons from individual NPs passing through a tiny focal volume of typically 1 fL (10^{-15} l), from which the NP size can be calculated *via* autocorrelation analysis [21,22]. As with DLS, the size information comprises both the core and the ligand layer. Other techniques to determine NP size include nanoparticle tracking analysis (NTA) [23], atomic force microscopy (AFM) [24], absorption spectroscopy [25] and analytical ultracentrifugation [26]. Advantages as well as limitations of the different techniques are summarized in Table 1.

One should be aware that NP preparations are often polydisperse. The DLS technique directly provides the size distribution information. Still, one has to be careful when interpreting the data because DLS is based on density-density correlations and, therefore, the intensity scales with the sixth power of the NP diameter. Caution is advised when dealing with samples containing particles of markedly different sizes. Size distributions may also be quantified by using AFM. Such data have been proposed to be more accurate than those obtained via DLS [27]. TEM image analysis suffers from limited sampling, so that the selected NPs may not be representative of the whole sample. Overall, it is advisable to apply different methods to ensure a robust size determination.

Independent of the technique chosen for size characterization, the NPs should – if at all possible – be suspended in the medium/solvent that will be used to expose the NPs to the biological samples during such measurements. The colloidal stability of NP suspensions is influenced by many factors including the solution ionic strength, pH and solvent composition. Because NPs are often charge-stabilized, the colloidal stability of NPs in pure water is significantly different from that in biologically relevant media [28,29]. Particularly, one has to be aware that biomolecules present in biological media, such as proteins, will inevitably adsorb on the NP surface [30-32], which leads to an increase in the hydrodynamic radius of the NP. In fact, the NP size may even influence the characteristics of the protein corona [33-36], such as thickness, composition and protein activity, which may modulate their cellular interactions.

NP size effects on active cellular internalization

Endocytosis is a fundamental biological process used by cells to internalize (bio)molecules and, because of their similar size, also NPs [37,38]. It may involve the engagement of either clathrin or caveolin pits, but may also be independent of these proteins. As is apparent from the studies listed in Table 2, NP size may affect the uptake efficiency and kinetics, the internalization mechanism and also the subcellular distribution. A size-dependent uptake in different cell lines has been observed for Au [29,39,40], mesoporous silica [41], polystyrene [42] and iron oxide NPs [43], with the maximum cellular uptake at a NP core size in the range of 30–50 nm, which suggests that there is an optimal size for active uptake.

Hökstra *et al.* [59] used a range of fluorescent latex beads of defined sizes (50 – 1,000 nm) to investigate the effect of NP size on the entry pathway in non-phagocytic B16 cells. Internalization of NPs <200 nm was observed to involve clathrin-coated pits. With increasing size, a shift towards caveolae-mediated internalization became apparent, which turned out to be the predominant entry route for 500-nm particles. Rafailovich *et al.* [50] reported that 45-nm Au NPs penetrated cells via clathrin-mediated endocytosis, while the smaller 13-nm NPs entered mostly via phagocytosis.

By using spinning disk confocal microscopy and quantitative image analysis, Nienhaus and coworkers have systematically investigated the uptake of various NPs in the range of 3.3 – 100 nm by live HeLa cells. Interestingly, QDs [60] and Au nanoclusters (AuNCs) [61,62] with less than 10 nm diameter were found to accumulate on the plasma membrane before gradually entering the intracellular region (Figure 2). In stark contrast, large polystyrene NPs (100 nm) were directly internalized without detectable prior accumulation at the plasma

Table 1 Commonly used experimental techniques to characterize NP size

Technique	Advantages	Limitations
TEM	Direct visualization, high resolution	NP aggregation during sample preparation, electron beam damage, preference for electron-dense atomic species
DLS	Size distribution information available, fast, simple	Signal dominated by larger NPs, interference from luminescent species
NTA	Real time analysis, particle-by-particle measurement	Suitable to a certain size range, interference from luminescent species
FCS	High sensitivity, small sample volume, particle-by-particle measurement	NPs need to be luminescent, sensitive to aggregates
AFM	High size resolution, 3-D profile	Slow speed, limited scanning area
Absorption spectra	Simple, fast	Applicable to plasmonic (Au, Ag) and semiconductor (CdSe, CdTe) NPs
Analytical ultracentrifugation	Size distribution information available, high size resolution	Density of NPs needs to be known, long measurement time

Abbreviations used: TEM transmission electron microscopy, DLS dynamic light scattering, NTA nanoparticle tracking analysis, FCS fluorescence correlation spectroscopy, AFM atomic force microscopy.

Table 2 Size dependence of active cellular NP uptake

| NPs	Size (nm Ø)	Cell lines	Techniques	Main conclusions	Ref.
Au	2–15	MCF-7	ICP-MS, TEM	Higher uptake of smaller NPs; 2/6 nm locate in cytoplasm and nucleus, 15 nm only in cytoplasm	[44]
QDs	2–7	A-427	FCS	Size-dependent internalization efficiency	[45]
Au	2.4–89	Cos 1	Silver staining, CLSM	2.4 nm: in nucleus; 5.5 and 8.2 nm: partially in cytoplasm; 16 nm and above: no uptake	[46]
Au	2–100	SK-BR-3	CLSM	40/50 nm: greatest effect	[47]
Au	4–17	HeLa	AFM	Uptake increases with NP size	[48]
TiO$_2$	5–80	A549	Light scattering μ-Raman, TEM	Uptake depends on overall size (with hard corona)	[49]
Iron oxide	8–65	RAW264.7	ICP-AES	37 nm (HD 100 nm): highest uptake	[43]
Au	10–50	NRK	TEM, ICP-MS	Uptake efficiency: 50 > 25 > 10 nm	[44]
Au	13, 45	CF-31	TEM, SEM, CLSM	45 nm: clathrin-mediated endocytosis, 13 nm: mostly phagocytosis	[50]
Au	14–100	HeLa	ICP-AES, TEM	50 nm: maximum uptake	[39]
Au	15–55	SK-BR-3	SEM, ICP-MS,	Surface ligands affect size dependency	[51]
Au	15–90	J774A.1	ICP-AES	No significant size dependency	[52]
Au	16–58	RAW 264.7, HepG2	ICP-MS, TEM	Negatively charged: 40 nm highest uptake; positively charged: no size-dependent uptake	[53]
Au	20–80	CHO-K1, HeLa, MCF-7	Flow cytometry, ICP-AES, TEM,	Less internalization with increasing size	[54]
PS	20–100	1321 N1, A549	CLSM, flow cytometry	40 nm: fastest internalization rate	[42]
MSN	30–280	HeLa	CLSM, ICP-MS	50 nm: maximum uptake	[41]
Au	30–90	PC3	TEM, ICP-MS	50 nm: maximum uptake	[29]
SiO$_2$	32, 83	Caco-2	CLSM	32 nm: enter nucleus, migrate faster	[55]
PS	40–2000	HeLa, A549, 1321 N1, HCMEC D3, RAW 264.7	CLSM, flow cytometry	Uptake highly size-dependent for all cell lines, larger NPs enter more slowly	[56]
Au	45–110	CL1-0, HeLa	Scattering imaging	45 nm: maximum uptake	[40]
polymer	50–300	Caco-2, HT-29	Deserno's model, CLSM	100 nm: maximum uptake	[57]
polymer	150–500	L02, SMMC-7221	Fluorimetry	Large NPs with high net charge: uptake more efficient	[58]

Abbreviations used: *ICP-MS* inductively coupled plasma mass spectrometry, *CLSM* confocal laser scanning microscopy, *ICP-AES* inductively coupled plasma atomic emission spectrometry, *SEM* scanning electron microscopy, *MSN* mesoporous silica nanoparticles.

membrane (Figure 2) [63,64]. Lunov *et al.* [65] demonstrated that, despite having the same size, ~100-nm carboxy (PS-COOH) and amino functionalized polystyrene (PS-NH$_2$) NPs were internalized by human macrophages and by undifferentiated and PMA-differentiated monocytic THP-1 cells via different mechanisms. Notably, the mechanism did not only depend on the NP type and the cell type, but also on the experimental conditions (buffer or medium supplemented with human serum). They also noticed that only the PS-NH$_2$ NPs triggered NLRP3 inflammasome activation and subsequent release of pro-inflammatory interleukin 1β (IL-1β) by human macrophages [66]. Hühn *et al.* [67] modified colloidal AuNPs with amphiphilic polymers to obtain NPs with identical physical properties except for the sign of the charge

(negative/positive) and showed that the uptake rate by cells was higher for positively than for negatively charged NPs.

The size-dependent interaction of NPs with the cell membrane is likely related to the membrane-wrapping process that initiates receptor-mediated endocytosis. It requires the concerted formation of multiple NP-receptor interactions [68,69]. Small NPs have less ligand-to-receptor interactions than larger ones; thus, several small NPs need to interact simultaneously with receptors in close proximity to trigger membrane wrapping. In contrast, an individual, large NP can act as a cross-linking agent to cluster receptors and induce uptake. Mathematical modeling has demonstrated that receptor-mediated endocytosis is optimal when there is
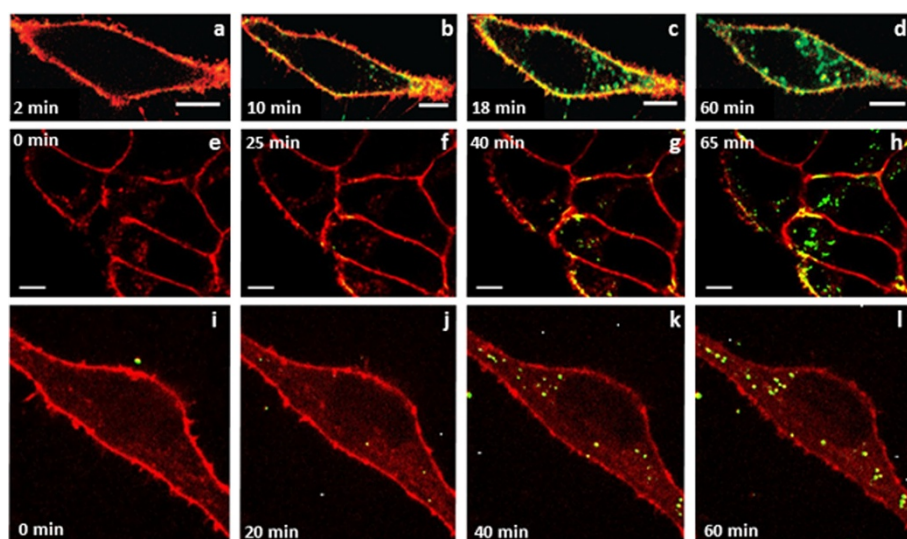
Figure 2 Active NP uptake. (a – d) Internalization of DPA-QDs (8 nm) by HeLa cells [60]. **(e – h)** Uptake of DHLA-AuNCs (3.3 nm) by HeLa cells [61]. **(i – l)** Uptake of polystyrene NPs (100 nm, coated with carboxylic groups) by mesenchymal stem cells (MSCs) [63]. Reproduced with permission from the American Chemical Society and the Royal Chemical Society.

no ligand shortage on the NP and no localized receptor shortage on the cell surface [70]. Thermodynamically, a 50 – 60 nm NP is capable of recruiting enough receptors to successfully trigger internalization. The nature of the protein corona, which is controlled by the NP surface ligands, may also affect the membrane response and, thereby, modify the cellular responses toward the NPs [52,71]. Considering that most uptake studies involving live cells have been performed in cell culture media supplemented with protein mixtures in varying compositions, it is not surprising that apparently 'identical' studies in some cases yielded conflicting results.

The size – as well the coating – can also influence the subcellular distribution of the internalized NPs. Lovrić *et al.* [72] demonstrated that positively charged 5.2-nm CdTe QDs were distributed throughout the cytoplasm of N9 cells but did not enter the nucleus, whereas positively charged 2.2-nm QDs were localized predominantly in the nuclear compartment. In contrast, Parak *et al.* [73] found that the size of the silica-coated QDs (8 and 16 nm, functionalized with thiols, amines or mercaptopropionic acid) did not influence the intracellular distribution. Oh *et al.* [46] investigated the cellular uptake of AuNPs coated with a cell-penetrating peptide. They reported that the ultimate intracellular destination was governed by the AuNP diameter. While the smallest, 2.4-nm AuNPs were found to localize to the nucleus, intermediate, 5.5- and 8.2-nm particles remained sequestered within the endolysosomal system. The 16-nm and larger AuNPs did not enter the cells on the experimental time scale, which is at variance with other reports (see Table 2).

These few examples already show the wide range of conclusions that can be drawn from NP uptake data. A dependence on one particular physicochemical parameter, *e.g.*, the core material of a core-shell NP, can be measured only if all other parameters are kept constant. There are only a few studies so far where this rule was strictly obeyed.

NP size effects on passive uptake

Red blood cells (RBCs) lack a cell nucleus, most organelles and, most importantly, the endocytic machinery [74]. Therefore, they have become valuable as a model system to investigate passive NP uptake. In 2005, Geiser *et al.* [75] analyzed the uptake of PS-NPs by RBCs and found that <200-nm but not 1-μm NPs enter RBCs. Rothen-Rutishauser and coworkers [76] refined the study and exposed RBCs to NPs of different material, size and surface charge (Table 3), and visualized them inside RBCs using confocal laser scanning microscopy (CLSM) in combination with digital data restoration, conventional TEM, and energy filtering TEM. A quantitative analysis revealed that only the size determined the uptake efficiency. They confirmed that particles <200 nm enter RBCs. The overall numbers were extremely small, however, with less than 1 particle per cell on average.

Zhao *et al.* [79] investigated the interactions of mesoporous silica nanoparticles (MSNs) having different sizes and surface properties with RBC membranes using membrane filtration, flow cytometry, and various microscopic techniques to evaluate their potential for intravenous drug delivery. The study focused on the first step of NP uptake, *i.e.*, the interaction of the NPs with the cell membrane. Small MCM-41-type MSNs (~100 nm)

Table 3 Size dependence of passive cellular NP uptake

NPs	Size (nm Ø)	Bio-system	Techniques	Main conclusions	Ref
DPA-QDs	8	RBCs	CLSM, SEIRAS	QDs penetrate cell membranes without pore formation	[77]
MSNs	100–300	RBCs	TEM	Hemolytic properties of MSNs related to silanol groups accessible to the cell membranes	[78]
MSNs	100–600	RBCs	CLSM, TEM	Strongly dependent on surface chemistry and NP size	[79]
PS	78–2,000	RBCs	CLSM	NPs < 0.2 μm enter RBCs	[75]
PS	2–1,000	RBCs	CLSM, TEM	Surface charge and NP composition do not influence entry, NPs < 0.2 μm enter RBCs, size is key factor for internalization by RBCs	[76]
Au	25–1,000				
TiO$_2$	20–30				
HAP	14–175	RBCs	Optical microscopy, TEM	Surface charge more crucial than the size for NP-RBC interaction, NP adhesion led to invaginations on RBC membrane	[80]
Au	4–5	DC2.4	STM, CLSM	'Striped' NPs, decorated with alternating hydrophobic and hydrophilic ligands, penetrate cell membranes without generating transient holes	[81]

Abbreviations used: SEIRAS surface-enhanced infrared absorption spectroscopy, HAP hydroxyapatite.

adsorbed to the surface of RBCs without disturbing the membrane or the cell morphology (Figure 3). In contrast, adsorption of large SBA-15-type MSNs (~600 nm) induced strong local membrane deformations, followed by internalization of the particles and, eventually, hemolysis. The interactions of MSNs with the RBC membranes apparently depended on the presence of silanol groups on the particle surface because blocking these silanols with organic groups reduced their interactions with the RBC membranes.

Recently, Wang *et al.* [77] studied the interactions between 8-nm QDs coated with the small, zwitterionic amino acid ligand D-penicillamine (DPA) and RBCs. At neutral pH, the charges on the amino and carboxylic acid groups of the surface ligands are balanced. After incubation with 10 nM DPA-QDs in PBS solution for different time periods and separation of free DPA-QDs by centrifugation, the RBC cells were transferred to a microscope sample cell and imaged using confocal fluorescence microscopy. The data clearly showed that the
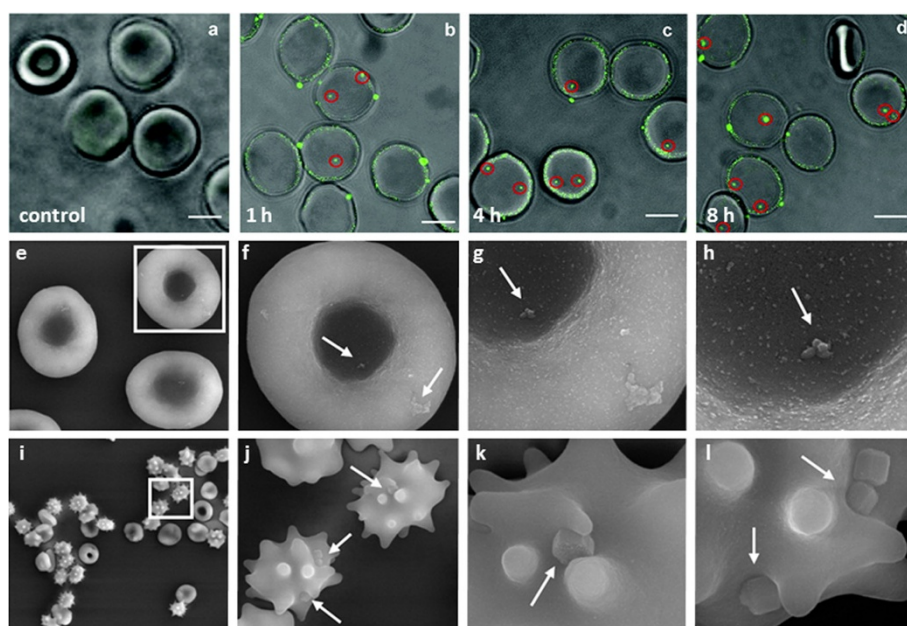
Figure 3 Passive NP uptake by red blood cells. (a – d) Internalization of DPA-QDs (8 nm) [77]. **(e – l)** Scanning electron micrographs (SEM) of RBCs (5% hematocrit) incubated with 100 μg mL^{-1} of **(e – h)** small (~100 nm) and **(i – l)** large (~600 nm) mesoporous silica particles (MSN) [79]. Reproduced with permission from the American Chemical Society.

DPA-QDs adhered to the RBC membranes, and the number of fluorescence spots, either close to the cell membranes or inside the cells, increased with exposure time (Figure 3). Moreover, the adsorbed DPA-QDs did not induce strong local membrane deformations. In fact, the RBC membranes remained largely intact during NP penetration of the bilayer, as evidenced by confocal microscopy images taken in the presence of calcein violet AM. This cell membrane-permeant dye becomes impermeant after entering the cell because of hydrolysis by intracellular esterases [81]. Surface-enhanced infrared absorption spectroscopy (SEIRAS) measurements carried out on model membrane preparations resembling RBC membranes revealed that the bilayer structure was softened in the presence of DPA-QDs, which may facilitate penetration of DPA-QDs into the lipid bilayer without causing poration.

The interaction of the NP with the membrane is arguably the most critical step in passive membrane penetration. Van Lehn *et al.* [82] proposed that, to avoid pore formation, the interaction should lead to fusion of the NP with the membrane. They suggested that fusion is highly favored when the ligand layer on the NP is able to easily fluctuate to adjust to the membrane, allowing surface charges to rearrange so that the NP appears locally hydrophobic. As the ligand layer around smaller particles contains a large amount of free volume because of the high curvature, ligand fluctuations are maximized so that small NPs should more easily penetrate a membrane. Certain small peptides [83,84] and synthetic nanomaterials such as carbon nanotubes [85] were found to be capable of crossing membranes without poration. The DPA monolayer of the QDs used by Wang *et al.* [77] resembles the pattern of hydrophobic and charged residues found in cell-penetrating peptides. Charged particles such as cationic QDs, however, typically induce transient poration of the cell membranes, which may result in cytotoxic effects [81].

NP size affects cytotoxicity upon internalization

A complete analysis of the pharmacokinetics of NPs has to include absorption of biomolecules, distribution, metabolism, and excretion [86]. A protein adsorption layer on the surface confers a new biological identity to the NP, which may completely modify the subsequent cellular and tissue responses, *e.g.*, the distribution to various organs, tissues, and cells. Once inside a cell or tissue, the surface layer, including the adsorbed biomolecules, and also the NP core
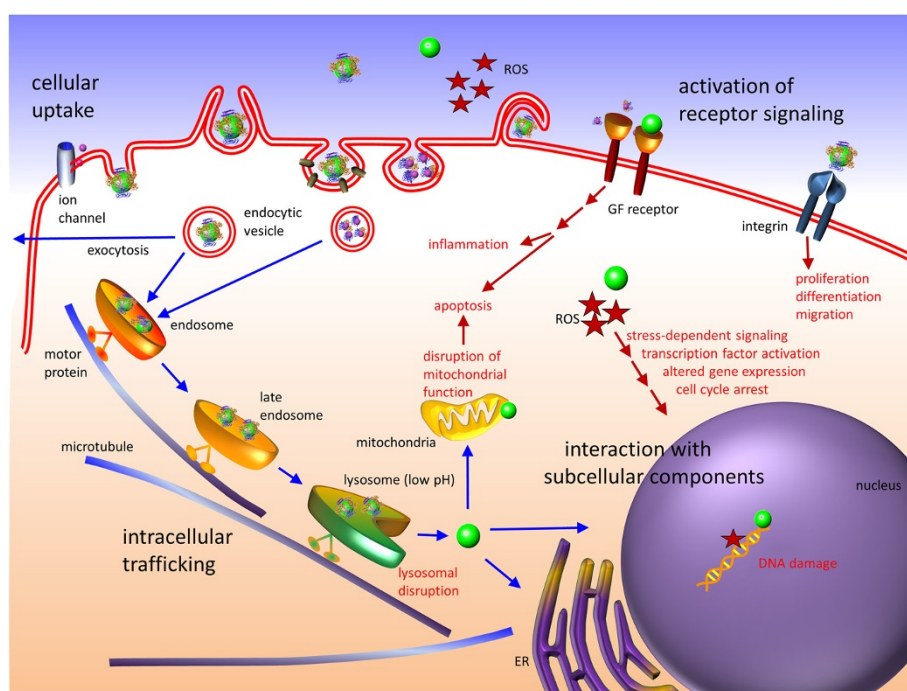
Figure 4 Cytotoxic effects of NPs. In the biological environment, NPs may trigger the production of reactive oxygen species (ROS). Elevated ROS levels may lead to (i) activation of cellular stress-dependent signaling pathways, (ii) direct damage of subcellular organelles such as mitochondria and (iii) DNA fragmentation in the nucleus, resulting in cell cycle arrest, apoptosis, and inflammatory response. NPs may interact with membrane-bound cellular receptors, *e.g.*, growth factor (GF) receptors and integrins, inducing cellular phenotypes such as proliferation, apoptosis, differentiation, and migration. After internalization via endocytic pathways, NPs are trafficked along the endolysosomal network within vesicles with the help of motor proteins and cytoskeletal structures. To access cytoplasmic or nuclear targets, NPs must escape from the endolysosomal network and traverse through the crowded cytoplasm.

material will likely be metabolized. Subsequently, the (remnants of the) NPs may be excreted by the organism. All these interactions with the biological environment are again dependent on the physicochemical properties of NPs including their size [87] (Figure 4). To evaluate the toxicity profile of NPs, two main approaches have been established: (i) functional assays assess the effects of NPs on cellular processes, (ii) viability assays probe whether the NPs cause death in a cell or a system of cells [88]. Although some aspects of size dependent NP toxicity may be reasonably well predicted by *in vitro* techniques, it remains difficult to judge whether the observed cytotoxicity is clinically relevant.

As can be inferred from the studies listed in Table 4, smaller NPs appear to be more toxic than larger ones. Small NPs possess a high surface area relative to their total mass, which increases the chance to interact with surrounding biomolecules and, as a consequence, to trigger adverse responses. Pan *et al.* [89] observed that small AuNPs (1.4 nm) were highly toxic and caused predominately rapid cell death by necrosis within 12 h, while larger, 15-nm AuNPs displayed low toxicity, irrespective of cell type and surface ligands. Likewise, 4-nm AgNPs were found to induce much higher levels ROS production and interleukin-8 secretion than 20- and 70-nm AgNPs at otherwise identical conditions [90]. A size dependent toxicity was also reported for SiO_2 [91] and

polymer NPs [92]. In contrast, the immunological responses of macrophages to AgNPs in the size range 3–25 nm were not significantly different, as inferred from the expression of the pro-inflammatory gene products interleukin-1, interleukin-6, and tumor necrosis factor [93]. Chen *et al.* [94] reported that Au NPs of 3, 5, 50, and 100 nm were nontoxic when injected intraperitoneally into mice, whereas Au NPs between 8 and 37 nm caused severe toxicity and death within 3 weeks. In HeLa cells, however, the same set of AuNPs was essentially non-toxic, regardless of size. The toxic effects in mice were less pronounced after coating the NP surface with peptides that induced an enhanced immune response. These apparently contradicting observations stress that caution is advised when it comes to drawing general conclusions on the *in-vivo* toxicity of a particular NP preparation from *in-vitro* data. In fact, the conditions under which nano-bio interactions take place in living organisms such as experimental mammals or humans are much more complex.

In summary, small NPs have a large, often catalytically active surface that may favor adverse chemical reactions such as ROS generation. Endocytosis mechanism, cellular uptake yield and efficiency of particle processing in the endocytic pathway also depend on the NP size [87]. In whole organisms, *e.g.*, mice, the *in-vivo* NP toxicity is

Table 4 Size-dependent cytotoxicity of NPs

NPs	Size (nm, Ø)	Cell lines	Evaluation techniques	Main conclusions	Ref
Au	0.8–15	SK-MEL-28, HeLa, L929, J774A1	TEM, MTT assays, FACS	Cytotoxicity depends on size, not ligand chemistry; small NPs more toxic	[89]
QDs	2.2, 5.2	PC12, N9	MTT assays	Smaller NPs more toxic	[72]
Au	5, 15	Balb/3 T3	Colony forming efficiency, Trypan Blue assays	5 nm, toxic; 15 nm, non-toxic	[95]
Au	3–38	J774 A1	Sizing and counting of cells	AuNPs, increased toxicity for larger NPs; AgNPs, no size-dependence in toxicity	[93]
Ag	3–25				
Au	10–25	HDMEC, A549, NCIH441	MTS assays, Ki-67 expression, LDH release	Size not a significant factor for cytotoxicity compared with surface ligands	[96]
Ag	15–55	F-12 K	MTT assays, LDH leakage, ROS production, MMP, inflammatory response	Increased toxicity for smaller NPs	[97]
Ag	4–70	U937	Cell viability, ROS production, cytokine release assays	Size-dependent toxicity (4 nm highest)	[90]
SiO_2	32, 83	Caco-2	WST-1 assays, comet assays	No cytotoxicity detected for either size	[55]
polymer	45, 90	NR8383, Caco-2	Mitochondrial membrane potential, ROS production, ATP depletion, TNF-α release	Positively charged 45-nm NPs more toxic than equally charged 90-nm NPs	[92]
Ag	10–100	MC3T3, PC12	Cell viability, ROS production, LDH release assays, gene expression, apoptosis detection	10 nm: greatest amount of apoptosis	[98]
TiO_2	14–196	osteoblasts, L-02, HEK 293	Alkaline phosphatase and zymography evaluation	Size-dependent cytotoxicity, 100 nm critical size	[99]
Au	20, 200	DU-145	MTS assays	Both sizes cytotoxic	[100]
SiO_2	50, 200	GT1-7	Counting cells, intracellular calcium homeostasis	200 nm: no toxic effects, 50 nm: toxicity with Ca level increase	[91]

Abbreviations used: MTT 3-(4,5-dimethylthiazol-2-yl)-2,5-diphenyltetrazolium bromide, FACS fluorescence-activated cell sorting, LDH lactate dehydrogenase, MTS (3-(4,5-dimethylthiazol-2-yl)-5-(3-carboxymethoxyphenyl)-2-(4-sulfophenyl)-2H-tetrazolium) tetrazolium, ROS Reactive Oxygen Species, MMP mitochondrial membrane potential, WST water-soluble tetrazolium salt.

directly related to the biodistribution and the retention times, which are both size-dependent. Overall, the harmfulness of NPs may closely correlate with their size-related ability to readily enter biological systems. However, size is not the only factor that governs toxicity; other factors such as surface functionalization also play important roles. For example, cationic NPs are considered more toxic than neutral or anionic ones, possibly due to their high affinity towards the negatively charged plasma membrane. Therefore, NP toxicity must be evaluated by changing NP properties systematically, one at a time.

Conclusions

In summary, the size of NPs has a strong effect on their interactions with living cells, influencing uptake efficiency, internalization pathway selection, intracellular localization and cytotoxicity. Despite huge efforts in this area, it still remains challenging to reliably correlate a particular cellular response with NP size. Considering the vast variety of nanomaterials and the complexity of the biological probes, it is difficult to draw general conclusions from the huge pool of available data. Still, we believe that there are a few general trends that can be trusted. (i) There is an optimal size for efficient endocytosis of NPs independent of the particle composition. (ii) This critical size can vary with cell type and surface properties of the NPs. (iii) Small NPs have a higher probability to be internalized by passive uptake than large ones. (iv) Under otherwise identical conditions, small NPs are more likely to cause toxic cellular responses.

Further research on NP-cell interactions will benefit from advances in the synthesis of well-defined, monodisperse NPs and the development of sophisticated analysis tools. We are confident that these efforts will result in a better understanding of the influence of physicochemical properties of nanomaterials on their interaction with biological systems and will provide guidelines to the design of more advanced biocompatible and efficient nanodevices.

Competing interests
The authors declare that they have no competing interests.

Authors' contributions
All authors have written and approved the final manuscript. They agree to be accountable for all aspects of the work in ensuring that questions related to the accuracy or integrity of any part of the work are appropriately investigated and resolved.

Author details
[1]Institute of Applied Physics and Center for Functional Nanostructures (CFN), Karlsruhe Institute of Technology (KIT), Wolfgang-Gaede-Strasse 1, 76131 Karlsruhe, Germany. [2]Institute of Toxicology and Genetics (ITG), Karlsruhe Institute of Technology (KIT), Hermann-von-Helmholtz-Platz 1, 76344 Eggenstein-Leopoldshafen, Germany. [3]Department of Physics, University of Illinois at Urbana-Champaign, Urbana, IL 61801, USA.

References
1. Astruc D: **Transition - metal nanoparticles in catalysis: from historical background to the state - of - the art.** In *Nanoparticles and Catalysis.* Edited by Astruc D. KGaA, Weinheim: WILEY-VCH Verlag GmbH & Co; 2008.
2. Saha K, Agasti SS, Kim C, Li XN, Rotello VM: **Gold nanoparticles in chemical and biological sensing.** *Chem Rev* 2012, **112**:2739–2779.
3. Stratakis E, Kymakis E: **Nanoparticle-based plasmonic organic photovoltaic devices.** *Mater Today* 2013, **16**:133–146.
4. Saroja C, Lakshmi P, Bhaskaran S: **Recent trends in vaccine delivery systems: a review.** *Int J Pharm Invest* 2011, **1**:64–74.
5. Meng FH, Cheng R, Deng C, Zhong ZY: **Intracellular drug release nanosystems.** *Mater Today* 2012, **15**:436–442.
6. Yoo JW, Irvine DJ, Discher DE, Mitragotri S: **Bio-inspired, bioengineered and biomimetic drug delivery carriers.** *Nat Rev Drug Discov* 2011, **10**:521–535.
7. Stark WJ: **Nanoparticles in biological systems.** *Angew Chem Int Ed* 2011, **50**:1242–1258.
8. Cheng LC, Jiang XM, Wang J, Chen CY, Liu RS: **Nano-bio effects: interaction of nanomaterials with cells.** *Nanoscale* 2013, **5**:3547–3569.
9. Röcker C, Pötzl M, Zhang F, Parak WJ, Nienhaus GU: **A quantitative fluorescence study of protein monolayer formation on colloidal nanoparticles.** *Nat Nanotechnol* 2009, **4**:577–580.
10. Jiang X, Weise S, Hafner M, Röcker C, Zhang F, Parak WJ, Nienhaus GU: **Quantitative analysis of the protein corona on FePt nanoparticles formed by transferrin binding.** *J R Soc Interface* 2010, **7**(Suppl 1):S5–S13.
11. Maffre P, Nienhaus K, Amin F, Parak WJ, Nienhaus GU: **Characterization of protein adsorption onto FePt nanoparticles using dual-focus fluorescence correlation spectroscopy.** *Beilstein J Nanotechnol* 2011, **2**:374–383.
12. Lynch I, Salvati A, Dawson KA: **Protein-nanoparticle interactions: what does the cell see?** *Nat Nanotechnol* 2009, **4**:546–547.
13. Lundqvist M, Stigler J, Cedervall T, Berggard T, Flanagan MB, Lynch I, Elia G, Dawson K: **The evolution of the protein corona around nanoparticles: a test study.** *ACS Nano* 2011, **5**:7503–7509.
14. Verma A, Stellacci F: **Effect of surface properties on nanoparticle-cell interactions.** *Small* 2010, **6**:12–21.
15. Mahmoudi M, Saeedi-Eslami SN, Shokrgozar MA, Azadmanesh K, Hassanlou M, Kalhor HR, Burtea C, Rothen-Rutishauser B, Laurent S, Sheibani S, Vali H: **Cell "vision": complementary factor of protein corona in nanotoxicology.** *Nanoscale* 2012, **4**:5461–5468.
16. Cho EC, Zhang Q, Xia Y: **The effect of sedimentation and diffusion on cellular uptake of gold nanoparticles.** *Nat Nanotechnol* 2011, **6**:385–391.
17. Li LW, Mu QX, Zhang B, Yan B: **Analytical strategies for detecting nanoparticle-protein interactions.** *Analyst* 2010, **135**:1519–1530.
18. Saptarshi S, Duschl A, Lopata A: **Interaction of nanoparticles with proteins: relation to bio-reactivity of the nanoparticle.** *J Nanobiotechnol* 2013, **11**:26.
19. Mahl D, Diendorf J, Meyer-Zaika W, Epple M: **Possibilities and limitations of different analytical methods for the size determination of a bimodal dispersion of metallic nanoparticles.** *Colloids Surf A* 2011, **377**:386–392.
20. Cho EJ, Holback H, Liu KC, Abouelmagd SA, Park J, Yeo Y: **Nanoparticle characterization: state of the art, challenges, and emerging technologies.** *Mol Pharm* 2013, **10**:2093–2110.
21. Zemanova L, Schenk A, Nienhaus GU, Valler MJ, Heilker R: **Confocal optics microscopy for biochemical and cellular high-throughput screening.** *Drug Discov Today* 2004, **9**:26–26.
22. Nienhaus GU, Maffre P, Nienhaus K: **Studying the protein corona on nanoparticles by FCS.** *Methods Enzymol* 2013, **519**:115–137.
23. Saveyn H, De Baets B, Thas O, Hole P, Smith J, Van der Meeren P: **Accurate particle size distribution determination by nanoparticle tracking analysis based on 2-D Brownian dynamics simulation.** *J Colloid Interf Sci* 2010, **352**:593–600.

24. Glatzel T, Hölscher H, Schimmel T, Baykara MZ, Schwarz UD, Garcia R: **Advanced atomic force microscopy techniques.** *Beilstein J Nanotechnol* 2012, **3**:893–894.

25. Haiss W, Thanh NTK, Aveyard J, Fernig DG: **Determination of size and concentration of gold nanoparticles from UV–vis spectra.** *Anal Chem* 2007, **79**:4215–4221.

26. Planken KL, Colfen H: **Analytical ultracentrifugation of colloids.** *Nanoscale* 2010, **2**:1849–1869.

27. Hoo C, Starostin N, West P, Mecartney M: **A comparison of atomic force microscopy (AFM) and dynamic light scattering (DLS) methods to characterize nanoparticle size distributions.** *J Nanopart Res* 2008, **10**:89–96.

28. MacCuspie R: **Colloidal stability of silver nanoparticles in biologically relevant conditions.** *J Nanopart Res* 2011, **13**:2893–2908.

29. Malugin A, Ghandehari H: **Cellular uptake and toxicity of gold nanoparticles in prostate cancer cells: a comparative study of rods and spheres.** *J Appl Toxicol* 2010, **30**:212–217.

30. Treuel L, Nienhaus G: **Toward a molecular understanding of nanoparticle–protein interactions.** *Biophys Rev* 2012, **4**:137–147.

31. Monopoli MP, Walczyk D, Campbell A, Elia G, Lynch I, Baldelli Bombelli F, Dawson KA: **Physical–chemical aspects of protein corona: relevance to in vitro and in vivo biological impacts of nanoparticles.** *J Am Chem Soc* 2011, **133**:2525–2534.

32. Shang L, Dörlich RM, Trouillet V, Bruns M, Nienhaus GU: **Ultrasmall fluorescent silver nanoclusters: protein adsorption and its effects on cellular responses.** *Nano Res* 2012, **5**:531–542.

33. Wang J, Jensen UB, Jensen GV, Shipovskov S, Balakrishnan VS, Otzen D, Pedersen JS, Besenbacher F, Sutherland DS: **Soft interactions at nanoparticles alter protein function and conformation in a size dependent manner.** *Nano Lett* 2011, **11**:4985–4991.

34. Tenzer S, Docter D, Rosfa S, Wlodarski A, Kuharev J, Rekik A, Knauer SK, Bantz C, Nawroth T, Bier C, et al: **Nanoparticle size is a critical physicochemical determinant of the human blood plasma corona: a comprehensive quantitative proteomic analysis.** *ACS Nano* 2011, **5**:7155–7167.

35. Shang W, Nuffer JH, Muniz-Papandrea VA, Colon W, Siegel RW, Dordick JS: **Cytochrome c on silica nanoparticles: influence of nanoparticle size on protein structure, stability, and activity.** *Small* 2009, **5**:470–476.

36. Tenzer S, Docter D, Kuharev J, Musyanovych A, Fetz V, Hecht R, Schlenk F, Fischer D, Kiouptsi K, Reinhardt C, et al: **Rapid formation of plasma protein corona critically affects nanoparticle pathophysiology.** *Nat Nanotechnol* 2013, **8**:772–781.

37. Iversen TG, Skotland T, Sandvig K: **Endocytosis and intracellular transport of nanoparticles: present knowledge and need for future studies.** *Nano Today* 2011, **6**:176–185.

38. Canton I, Battaglia G: **Endocytosis at the nanoscale.** *Chem Soc Rev* 2012, **41**:2718–2739.

39. Chithrani BD, Ghazani AA, Chan WCW: **Determining the size and shape dependence of gold nanoparticle uptake into mammalian cells.** *Nano Lett* 2006, **6**:662–668.

40. Wang SH, Lee CW, Chiou A, Wei PK: **Size-dependent endocytosis of gold nanoparticles studied by three-dimensional mapping of plasmonic scattering images.** *J Nanobiotechnol* 2010, **8**:33.

41. Lu F, Wu SH, Hung Y, Mou CY: **Size effect on cell uptake in well-suspended, uniform mesoporous silica nanoparticles.** *Small* 2009, **5**:1408–1413.

42. Varela JA, Bexiga MG, Aberg C, Simpson JC, Dawson KA: **Quantifying size-dependent interactions between fluorescently labeled polystyrene nanoparticles and mammalian cells.** *J Nanobiotechnol* 2012, **10**:39.

43. Huang J, Bu L, Xie J, Chen K, Cheng Z, Li X, Chen X: **Effects of nanoparticle size on cellular uptake and liver MRI with polyvinylpyrrolidone-coated iron oxide nanoparticles.** *ACS Nano* 2010, **4**:7151–7160.

44. Huang K, Ma H, Liu J, Huo S, Kumar A, Wei T, Zhang X, Jin S, Gan Y, Wang PC, et al: **Size-dependent localization and penetration of ultrasmall gold nanoparticles in cancer cells, multicellular spheroids, and tumors in vivo.** *ACS Nano* 2012, **6**:4483–4493.

45. Dong C, Irudayaraj J: **Hydrodynamic size-dependent cellular uptake of aqueous QDs probed by fluorescence correlation spectroscopy.** *J Phys Chem B* 2012, **116**:12125–12132.

46. Oh E, Delehanty JB, Sapsford KE, Susumu K, Goswami R, Blanco-Canosa JB, Dawson PE, Granek J, Shoff M, Zhang Q, et al: **Cellular uptake and fate of PEGylated gold nanoparticles is dependent on both cell-penetration peptides and particle size.** *ACS Nano* 2011, **5**:6434–6448.

47. Jiang W, Kim BYS, Rutka JT, Chan WCW: **Nanoparticle-mediated cellular response is size-dependent.** *Nat Nanotechnol* 2008, **3**:145–150.

48. Shan Y, Ma S, Nie L, Shang X, Hao X, Tang Z, Wang H: **Size-dependent endocytosis of single gold nanoparticles.** *Chem Commun* 2011, **47**:8091–8093.

49. Andersson PO, Lejon C, Ekstrand-Hammarstrom B, Akfur C, Ahlinder L, Bucht A, Osterlund L: **Polymorph- and size-dependent uptake and toxicity of TiO(2) nanoparticles in living lung epithelial cells.** *Small* 2011, **7**:514–523.

50. Mironava T, Hadjiargyrou M, Simon M, Jurukovski V, Rafailovich MH: **Gold nanoparticles cellular toxicity and recovery: effect of size, concentration and exposure time.** *Nanotoxicology* 2010, **4**:120–137.

51. Cho EC, Au L, Zhang Q, Xia Y: **The effects of size, shape, and surface functional group of gold nanostructures on their adsorption and internalization by cells.** *Small* 2010, **6**:517–522.

52. Walkey CD, Olsen JB, Guo H, Emili A, Chan WC: **Nanoparticle size and surface chemistry determine serum protein adsorption and macrophage uptake.** *J Am Chem Soc* 2012, **134**:2139–2147.

53. Liu X, Huang N, Li H, Jin Q, Ji J: **Surface and size effects on cell interaction of gold nanoparticles with both phagocytic and nonphagocytic cells.** *Langmuir* 2013, **29**:9138–9148.

54. Elbakry A, Wurster EC, Zaky A, Liebl R, Schindler E, Bauer-Kreisel P, Blunk T, Rachel R, Goepferich A, Breunig M: **Layer-by-layer coated gold nanoparticles: size-dependent delivery of DNA into cells.** *Small* 2012, **8**:3847–3856.

55. Schübbe S, Schumann C, Cavelius C, Koch M, Müller T, Kraegeloh A: **Size-dependent localization and quantitative evaluation of the intracellular migration of silica nanoparticles in caco-2 cells.** *Chem Mater* 2012, **24**:914–923.

56. dos Santos T, Varela J, Lynch I, Salvati A, Dawson KA: **Quantitative assessment of the comparative nanoparticle-uptake efficiency of a range of cell lines.** *Small* 2011, **7**:3341–3349.

57. Xu A, Yao M, Xu G, Ying J, Ma W, Li B, Jin Y: **A physical model for the size-dependent cellular uptake of nanoparticles modified with cationic surfactants.** *Int J Nanomedicine* 2012, **7**:3547–3554.

58. He C, Hu Y, Yin L, Tang C, Yin C: **Effects of particle size and surface charge on cellular uptake and biodistribution of polymeric nanoparticles.** *Biomaterials* 2010, **31**:3657–3666.

59. Rejman J, Oberle V, Zuhorn IS, Hoekstra D: **Size-dependent internalization of particles via the pathways of clathrin- and caveolae-mediated endocytosis.** *Biochem J* 2004, **377**:159–169.

60. Jiang X, Röcker C, Hafner M, Brandholt S, Dörlich RM, Nienhaus GU: **Endo- and exocytosis of zwitterionic quantum dot nanoparticles by live HeLa cells.** *ACS Nano* 2010, **4**:6787–6797.

61. Yang L, Shang L, Nienhaus GU: **Mechanistic aspects of fluorescent gold nanocluster internalization by live HeLa cells.** *Nanoscale* 2013, **5**:1537–1543.

62. Shang L, Stockmar F, Azadfar N, Nienhaus GU: **Intracellular thermometry by using fluorescent gold nanoclusters.** *Angew Chem Int Ed Engl* 2013, **52**:11154–11157.

63. Jiang X, Dausend J, Hafner M, Musyanovych A, Röcker C, Landfester K, Mailänder V, Nienhaus GU: **Specific effects of surface amines on polystyrene nanoparticles in their interactions with mesenchymal stem cells.** *Biomacromolecules* 2010, **11**:748–753.

64. Jiang X, Musyanovych A, Röcker C, Landfester K, Mailänder V, Nienhaus GU: **Specific effects of surface carboxyl groups on anionic polystyrene particles in their interactions with mesenchymal stem cells.** *Nanoscale* 2011, **3**:2028–2035.

65. Lunov O, Syrovets T, Loos C, Beil J, Delacher M, Tron K, Nienhaus GU, Musyanovych A, Mailänder V, Landfester K, Simmet T: **Differential uptake of functionalized polystyrene nanoparticles by human macrophages and a monocytic cell line.** *ACS Nano* 2011, **5**:1657–1669.

66. Lunov O, Syrovets T, Loos C, Nienhaus GU, Mailänder V, Landfester K, Rouis M, Simmet T: **Amino-functionalized polystyrene nanoparticles activate the NLRP3 inflammasome in human macrophages.** *ACS Nano* 2011, **5**:9648–9657.

67. Hühn D, Kantner K, Geidel C, Brandholt S, De Cock I, Soenen SJ, Rivera Gil P, Montenegro JM, Braeckmans K, Mullen K, et al: **Polymer-coated nanoparticles interacting with proteins and cells: focusing on the sign of the net charge.** *ACS Nano* 2013, **7**:3253–3263.

68. Albanese A, Tang PS, Chan WC: **The effect of nanoparticle size, shape, and surface chemistry on biological systems.** *Annu Rev Biomed Eng* 2012, **14**:1–16.

69. Lunov O, Zablotskii V, Syrovets T, Röcker C, Tron K, Nienhaus GU, Simmet T: Modeling receptor-mediated endocytosis of polymer-functionalized iron oxide nanoparticles by human macrophages. *Biomaterials* 2011, **32**:547–555.

70. Yuan H, Li J, Bao G, Zhang S: Variable nanoparticle-cell adhesion strength regulates cellular uptake. *Phys Rev Lett* 2010, **105**:138101.

71. Shang L, Yang L, Seiter J, Heinle M, Brenner-Weiss G, Gerthsen D, Nienhaus GU: Nanoparticles interacting with proteins and cells: a systematic study of protein surface charge effects. *Adv Mater Interfaces* 2014. 10.1002/admi.201300079.

72. Lovrić J, Bazzi H, Cuie Y, Fortin GA, Winnik F, Maysinger D: Differences in subcellular distribution and toxicity of green and red emitting CdTe quantum dots. *J Mol Med* 2005, **83**:377–385.

73. Parak WJ, Boudreau R, Le Gros MA, Gerion D, Zanchet D, Micheel CM, Williams SC, Alivisatos AP, Larabell C: Cell motility and metastatic potential studies based on quantum dot imaging of phagokinetic tracks. *Adv Mater* 2002, **14**:882–885.

74. Underhill DM, Ozinsky A: Phagocytosis of microbes: complexity in action. *Annu Rev Immunol* 2002, **20**:825–852.

75. Geiser M, Rothen-Rutishauser B, Kapp N, Schurch S, Kreyling W, Schulz H, Semmler M, Im Hof V, Heyder J, Gehr P: Ultrafine particles cross cellular membranes by nonphagocytic mechanisms in lungs and in cultured cells. *Environ Health Perspect* 2005, **113**:1555–1560.

76. Rothen-Rutishauser BM, Schurch S, Haenni B, Kapp N, Gehr P: Interaction of fine particles and nanoparticles with red blood cells visualized with advanced microscopic techniques. *Environ Sci Technol* 2006, **40**:4353–4359.

77. Wang T, Bai J, Jiang X, Nienhaus GU: Cellular uptake of nanoparticles by membrane penetration: a study combining confocal microscopy with FTIR spectroelectrochemistry. *ACS Nano* 2012, **6**:1251–1259.

78. Slowing II, Wu CW, Vivero-Escoto JL, Lin VS: Mesoporous silica nanoparticles for reducing hemolytic activity towards mammalian red blood cells. *Small* 2009, **5**:57–62.

79. Zhao Y, Sun X, Zhang G, Trewyn BG, Slowing II, Lin VS: Interaction of mesoporous silica nanoparticles with human red blood cell membranes: size and surface effects. *ACS Nano* 2011, **5**:1366–1375.

80. Han Y, Wang X, Dai H, Li S: Nanosize and surface charge effects of hydroxyapatite nanoparticles on Red blood cell suspensions. *ACS Appl Mater Interfaces* 2012, **4**:4616–4622.

81. Verma A, Uzun O, Hu Y, Han HS, Watson N, Chen S, Irvine DJ, Stellacci F: Surface-structure-regulated cell-membrane penetration by monolayer-protected nanoparticles. *Nat Mater* 2008, **7**:588–595.

82. Van Lehn RC, Atukorale PU, Carney RP, Yang YS, Stellacci F, Irvine DJ, Alexander-Katz A: Effect of particle diameter and surface composition on the spontaneous fusion of monolayer-protected gold nanoparticles with lipid bilayers. *Nano Lett* 2013, **13**:4060–4067.

83. Koren E, Torchilin VP: Cell-penetrating peptides: breaking through to the other side. *Trends Mol Med* 2012, **18**:385–393.

84. Heitz F, Morris MC, Divita G: Twenty years of cell-penetrating peptides: from molecular mechanisms to therapeutics. *Br J Pharmacol* 2009, **157**:195–206.

85. Kostarelos K, Lacerda L, Pastorin G, Wu W, Wieckowski S, Luangsivilay J, Godefroy S, Pantarotto D, Briand JP, Muller S, *et al*: Cellular uptake of functionalized carbon nanotubes is independent of functional group and cell type. *Nat Nanotechnol* 2007, **2**:108–113.

86. Sharifi S, Behzadi S, Laurent S, Forrest ML, Stroeve P, Mahmoudi M: Toxicity of nanomaterials. *Chem Soc Rev* 2012, **41**:2323–2343.

87. Nel A, Xia T, Madler L, Li N: Toxic potential of materials at the nanolevel. *Science* 2006, **311**:622–627.

88. Love SA, Maurer-Jones MA, Thompson JW, Lin Y-S, Haynes CL: Assessing nanoparticle toxicity. *Annu Rev Anal Chem* 2012, **5**:181–205.

89. Pan Y, Neuss S, Leifert A, Fischler M, Wen F, Simon U, Schmid G, Brandau W, Jahnen-Dechent W: Size-dependent cytotoxicity of gold nanoparticles. *Small* 2007, **3**:1941–1949.

90. Park J, Lim DH, Lim HJ, Kwon T, Choi JS, Jeong S, Choi IH, Cheon J: Size dependent macrophage responses and toxicological effects of Ag nanoparticles. *Chem Commun* 2011, **47**:4382–4384.

91. Ariano P, Zamburlin P, Gilardino A, Mortera R, Onida B, Tomatis M, Ghiazza M, Fubini B, Lovisolo D: Interaction of spherical silica nanoparticles with neuronal cells: size-dependent toxicity and perturbation of calcium homeostasis. *Small* 2011, **7**:766–774.

92. Bhattacharjee S, Ershov D, Fytianos K, van der Gucht J, Alink GM, Rietjens IMCM, Marcelis ATM, Zuilhof H: Cytotoxicity and cellular uptake of tri-block copolymer nanoparticles with different size and surface characteristics. *Part Fibre Toxicol* 2012, **9**:11.

93. Yen HJ, Hsu SH, Tsai CL: Cytotoxicity and immunological response of gold and silver nanoparticles of different sizes. *Small* 2009, **5**:1553–1561.

94. Chen YS, Hung YC, Liau I, Huang GS: Assessment of the in vivo toxicity of gold nanoparticles. *Nanoscale Res Lett* 2009, **4**:858–864.

95. Coradeghini R, Gioria S, Garcia CP, Nativo P, Franchini F, Gilliland D, Ponti J, Rossi F: Size-dependent toxicity and cell interaction mechanisms of gold nanoparticles on mouse fibroblasts. *Toxicol Lett* 2013, **217**:205–216.

96. Freese C, Uboldi C, Gibson MI, Unger RE, Weksler BB, Romero IA, Couraud PO, Kirkpatrick CJ: Uptake and cytotoxicity of citrate-coated gold nanospheres: Comparative studies on human endothelial and epithelial cells. *Part Fibre Toxicol* 2012, **9**:23.

97. Carlson C, Hussain SM, Schrand AM K, Braydich-Stolle L, Hess KL, Jones RL, Schlager JJ: Unique cellular interaction of silver nanoparticles: size-dependent generation of reactive oxygen species. *J Phys Chem B* 2008, **112**:13608–13619.

98. Kim T-H, Kim M, Park H-S, Shin US, Gong M-S, Kim H-W: Size-dependent cellular toxicity of silver nanoparticles. *J Biomed Mater Res A* 2012, **100A**:1033–1043.

99. Cai K, Hou Y, Hu Y, Zhao L, Luo Z, Shi Y, Lai M, Yang W, Liu P: Correlation of the cytotoxicity of TiO_2 nanoparticles with different particle sizes on a sub-200-nm scale. *Small* 2011, **7**:3026–3031.

100. Vedantam P, Huang G, Tzeng TRJ: Size-dependent cellular toxicity and uptake of commercial colloidal gold nanoparticles in DU-145 cells. *Cancer Nanotechnol* 2013, **4**:13–20.